A method for estimating the critical Reynolds number for bypass transition in wall-bounded flows.

F. Laadhari
Laboratoire de Mécanique des Fluides et d'Acoustique
ERCOFTAC Workshop - ASTROFLU V

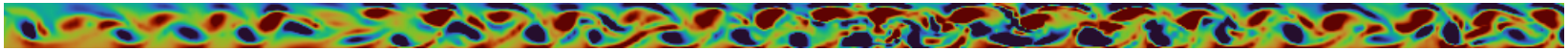

December 13, 2021

Study framework

- Present a method for estimating the critical Reynolds number for bypass transition in **canonical internal wall-bounded flows**: Plane Couette (PC), Plane Poiseuille (PP) and Pipe Flow (PF).
- Based on the integral of the mean-momentum transport equation: **the mean-moment turbulent flux as a function of centerline and friction velocities and Kármán number.**
- Critical Reynolds numbers can be estimated with the data from mean velocity profile in the turbulent regime.
- This allows predictions with good accuracy.
- Validated by direct numerical simulations (DNS) of a large aspect-ratio plane channel flow.

Background

Ten years after his seminal first paper on his famous experiment (Reynolds, 1883)► ◄ ,

- Reynolds (1895), by introducing the decomposition into mean and fluctuating fields in the Navier-Stokes equations,
- he attempted obtaining a criterion for the laminar-turbulent transition **in plane channel flow**.►

The Reynolds decomposition has been used since

- in statistical turbulence analysis in general
- or for stability studies around a base profile in particular.

But until now Reynolds-Averaged Navier-Stokes (RANS) équations have failed to provide any quantitative or qualitative information related to the sub-critical onset of turbulence.

Background

- *Although many advances have been made in understanding how turbulence in wall-bounded flows occurs, no progress has been made in connecting this transition to high Reynolds numbers fully-developed turbulent regime.(Barkley* et al.*, 2015)* and vice versa
- This study presents a method based on an exact relationship provided by bulk averaging of the Reynolds shear-stress obtained by integrating the RANS equations,▶
- namely, the evolution of the mean-momentum turbulent flux in canonical internal wall-bounded flows.

Background

With regard to the critical Reynolds number of the aforementioned flows, most of the studies agree on the following values:

	R_{τ_C}	R_{0_C}	R_{b_C}	Refs
(PC)	18	330 — 337	330 — 337	Bottin *et al.* (1998), Duguet *et al.* (2010)
(PP)	36	660	880	Xiong *et al.* (2015), Paranjape (2019)
(PF)	45 — 54	2020 — 2900	2020 — 2900	Avila *et al.* (2011), Eckhardt (2018)

▶Manneville (2015)

$R_\tau = \frac{h(\text{or}\, R) u_\tau}{\nu}$ being the Kármán number,

$R_0 = \frac{h(\text{or}\, R) U_C}{\nu}$ the Reynolds number based on the centerline velocity,

$R_b = \frac{2h(\text{or}\, D) U_b}{\nu}$ the bulk Reynolds number.

Background

Note that in pipe flow

- *It is difficult to know what the exact value of the critical Reynolds is because of extremely long equilibration times encountered and explain the wide scatter of the values of the critical point reported over the last 130 years* (Mukund & Hof, 2018).
- *The characteristic mean lifetime of the disturbances increases rapidly with Reynolds number and becomes inaccessibly large for Reynolds numbers exceeding about* 2250 (Faisst & Eckhardt, 2004).
- However, as suggested by Mellibovsky *et al.* (2009) and Barkley *et al.* (2015), the critical values of the bulk Reynolds number are in the interval $[2200, 2700]$, more limited than the one indicated in the previous table.

Notation and conventions

Notations

In what follows:

- The primed quantities correspond to fluctuations around the mean with u' and v' being the streamwise and wall-normal fluctuating velocities, respectively.
- The over-bar represents the one-point statistical averaged quantities.
- The brackets denote their space average (*1D or 2D*).
- The superscript $(+)$ indicates scaling with inner variables, i.e., ν the kinematic viscosity and u_τ the friction velocity defined from the wall viscous shear stress τ_w as $u_\tau = \sqrt{\tau_w/\rho}$, where ρ is the fluid density.
- R_τ is the Kármán number based on the friction velocity and the channel half-width h for plane Couette and plane Poiseuille flows and on the pipe radius R.

Notation and conventions

Plane Couette flow setup

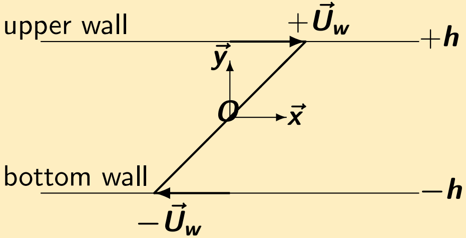

Plane Poiseuille setup

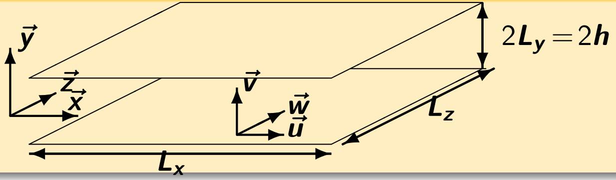

Notation and conventions

Pipe flow

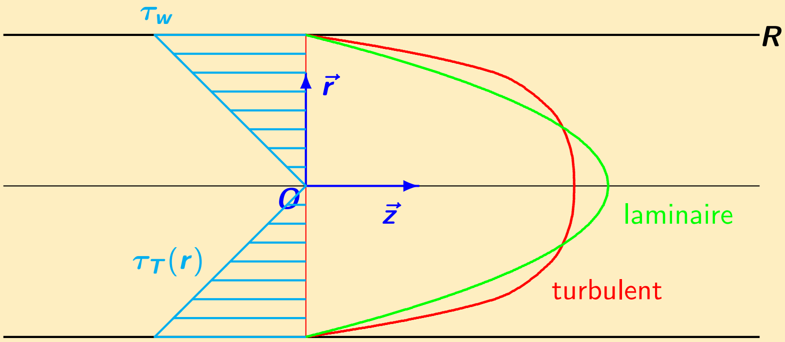

Equations

The bulk-averaging of the mean streamwise momentum equation for statistically steady and **2D** flow,i.e., $-\overline{u'v'}^{+} + \frac{\mathrm{d}\overline{U}^{+}}{\mathrm{d}y^{+}} = \frac{y}{h}$ leads to the following relations for the mean turbulent momentum flux over the gap $2h$ between the two moving wall, the half channel-width h, the pipe cross-section or the pipe radius:

$$-\left\langle \overline{u'v'}^{+} \right\rangle_{PC}^{2h} = 1 - \frac{\overline{U}_W^{+}}{R_\tau}$$

$\overline{U}_W$ the algebraic mean of wall velocities

$$-\left\langle \overline{u'v'}^{+} \right\rangle_{PP}^{h} = \frac{1}{2}\left(1 - 2\frac{\overline{U}_C^{+}}{R_\tau}\right)$$

$\overline{U}_C$ the mean centerline velocity

$$-\left\langle \overline{u'v'}^{+} \right\rangle_{PF}^{S} = \frac{2}{3}\left(1 - 3\frac{\overline{U}_R^{+}}{R_\tau}\right)$$

$\overline{U}_R$ the radius-averaged mean velocity

$$-\left\langle \overline{u'v'}^{+} \right\rangle_{PF}^{R} = \frac{1}{2}\left(1 - 2\frac{\overline{U}_B^{+}}{R_\tau}\right)$$

$\overline{U}_B$ the bulk mean velocity

Equations

These relations can be written in a generic manner:

$$-\left\langle \overline{\boldsymbol{u'v'}}^{+} \right\rangle = \boldsymbol{\alpha} \left(1 - \beta \frac{\boldsymbol{U}_0^+}{\boldsymbol{R_\tau}} \right), \text{ with}$$

- α the first coefficient in the right-hand members,
- $\boldsymbol{U}_0$ being the characteristic velocity and $\boldsymbol{U}_{0c}$ its laminar value.
- β the laminar value of the ratio $\boldsymbol{R_\tau}/\boldsymbol{U}_0^+$,i.e., $\beta = \boldsymbol{R_{\tau c}}/\boldsymbol{U}_{0c}^+$

flow type	α	β
$\boldsymbol{PC}$	1	1
$\boldsymbol{PP}\&\boldsymbol{PF^R}$	1/2	2
$\boldsymbol{PF^S}$	2/3	3

Conjecture

It is clear that this relation is verified in fully developed turbulent flows and also at the critical Kármán number at which the turbulence vanishes,i.e.,

$$\left\langle \overline{\boldsymbol{u'v'}}^{+} \right\rangle = 0,$$

when the product $\beta \boldsymbol{U}_0^+$ is equal to $\boldsymbol{R_\tau}$.

A question:

Could it be used to predict the critical values of table 1?

The answer is YES as it will be shown in the following.

DNS datasets

DNS datasets used in this study:

	Ref.	R_τ
PC	Pirozzoli *et al.* (2014)	170, 258, 509, <u>989</u>
	Avsarkisov *et al.* (2014)	131, 177, 243, 553
	Lee & Moser (2018)	93, 219, 501
PP	Hoyas & Jiménez (2006)	186, 546, 933, 2004
	Laadhari (2007)	72, 90, 120, 160, 180, 235, 395, 588, 1000
	Bernardini *et al.* (2014)	183, 550, 998, 2021, 4079
	Lee & Moser (2015)	182, 235, 543, 1000, 1994, <u>5186</u>
	Yamamoto & Tsuji (2018)	996, 1993, 3982
PF	Wu & Moin (2008)	181, 684, 1142
	El-Khoury *et al.* (2013)	181, 361, 550
	Chin *et al.* (2014)	171, 500, 2003
	Bauer *et al.* (2017)	1500
	Pirozzoli *et al.* (2021)	180, 495, 1136, 1976, 3028, <u>6019</u>

DNS datasets

New DNS of plane Poiseuille flow

- New DNS in large aspect-ratio rectangular duct are performed with a pseudo-spectral code (Buffat *et al.*, 2011).
- The computational domain has a size of $\boldsymbol{L_x} \times 2\boldsymbol{h} \times \boldsymbol{L_z}$, where streamwise dimension $\boldsymbol{L_x}$ and spanwize dimension $\boldsymbol{L_z}$ are typically $500\boldsymbol{h}$ and $250\boldsymbol{h}$, respectively.
- The resolution of the simulations is $2304 \times 129 \times 2304$ grid points.
- The Kármán number is in the range $36 \leqslant \boldsymbol{R_\tau} \leqslant 72$.
- The numerical experiments start from a fully developed turbulent flow and the Reynolds number is stepwisely decreased,
- after every step the statistics are computed over a statistically steady state.

Results

Plane Poiseuille flow

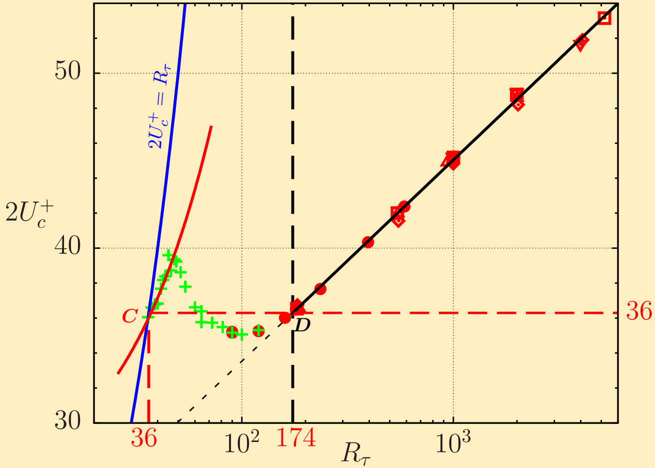

►Evolution of $2\boldsymbol{U_C^+}$ with $\boldsymbol{R_\tau}$ for PP flow, (+) present DNS.

Results

Plane Poiseuille flow

This figure shows that

- The laminar regime is reached at point $\boldsymbol{C}$ where $2\overline{\boldsymbol{U}}_{\boldsymbol{C}}^{+} = \boldsymbol{R}_{\boldsymbol{\tau}} \Rightarrow$ the critical Kármán value $\boldsymbol{R}_{\boldsymbol{\tau c}} = 36$.
- The critical value $2\overline{\boldsymbol{U}}_{\boldsymbol{C}c}^{+}$ is also reached at the turbulent point $\boldsymbol{D}$ with $\boldsymbol{R}_{\boldsymbol{\tau}_{\boldsymbol{D}}} = 174$,
- and at another point located between the previous ones.
- Near the point $\boldsymbol{C}$ the centerline velocity is well described by

$$\overline{\boldsymbol{U}}_{\boldsymbol{C}}^{+} = 12.57\left(1 - \frac{\boldsymbol{R}_{\boldsymbol{\tau}}}{\boldsymbol{R}_{\boldsymbol{\tau c}}}\right) + \frac{\boldsymbol{R}_{\boldsymbol{\tau}}}{2} \quad (2)$$

for $36 \leqslant \boldsymbol{R}_{\boldsymbol{\tau}} \leqslant 48$ with a relative departure (RD) in the range $\pm 1\%$

Results

Plane Poiseuille flow

- For $\boldsymbol{R_\tau} \geqslant \boldsymbol{R_{\tau_D}}$ it is well described by the logarithmic law

$$\overline{\boldsymbol{U}}^+_{\boldsymbol{C}} = 2.5 \ln \boldsymbol{R_\tau} + 5.25 \text{ (Laadhari, 2019)}$$

  with a RD in the range $\pm 1\%$.

- Then $\overline{\boldsymbol{U}}^+_{\boldsymbol{C}} = \frac{1}{\boldsymbol{\kappa}} \ln\left(\frac{\boldsymbol{R_\tau}}{\boldsymbol{A}}\right) = \frac{1}{\boldsymbol{\kappa}} \ln\left(\frac{\boldsymbol{R_{\tau_D}}}{\boldsymbol{A}}\right) + \frac{1}{\boldsymbol{\kappa}} \ln\left(\frac{\boldsymbol{R_\tau}}{\boldsymbol{R_{\tau_D}}}\right)$
  with $\boldsymbol{\kappa} = 0.4$ the von Kármán constant, $\boldsymbol{A} = 0.122$ and $\boldsymbol{R_{\tau_D}} = 174$.

- Since $\overline{\boldsymbol{U}}^+_{\boldsymbol{C_D}} = \overline{\boldsymbol{U}}^+_{\boldsymbol{C_C}} = \frac{\boldsymbol{R_{\tau_C}}}{2} = \frac{1}{\boldsymbol{\kappa}} \ln\left(\frac{\boldsymbol{R_{\tau_D}}}{\boldsymbol{A}}\right)$

$$\Rightarrow \overline{\boldsymbol{U}}^+_{\boldsymbol{C}} = \frac{\boldsymbol{R_{\tau_C}}}{2} + \frac{1}{\boldsymbol{\kappa}} \ln\left(\frac{\boldsymbol{R_\tau}}{\boldsymbol{R_{\tau_D}}}\right)$$

Results

Plane Poiseuille flow

et voilà

$$-\left\langle \overline{\boldsymbol{u'v'}}^{+} \right\rangle_{\boldsymbol{PP}}^{\boldsymbol{h}} = \frac{1}{2}\left[1 - \frac{\boldsymbol{R_{\tau C}}}{\boldsymbol{R_{\tau}}} - \frac{2}{\kappa \boldsymbol{R_{\tau}}} \ln\left(\frac{\boldsymbol{R_{\tau}}}{\boldsymbol{R_{\tau D}}}\right)\right] \qquad (3)$$

where the only unknown is $\boldsymbol{R_{\tau C}}$.

- Then, with $\boldsymbol{R_{\tau}} = \boldsymbol{R_{\tau D}}$, $\boldsymbol{R_{\tau C}} = 174 \times (1 - 2 \times 0.396) = 36.2$
- The fitting to this relation of the PP DNS dataset leads to the critical Kármán number $\boldsymbol{R_{\tau C}} = 36.3$
- 1% higher than the value obtained from the DNS.

Plane Poiseuille flow

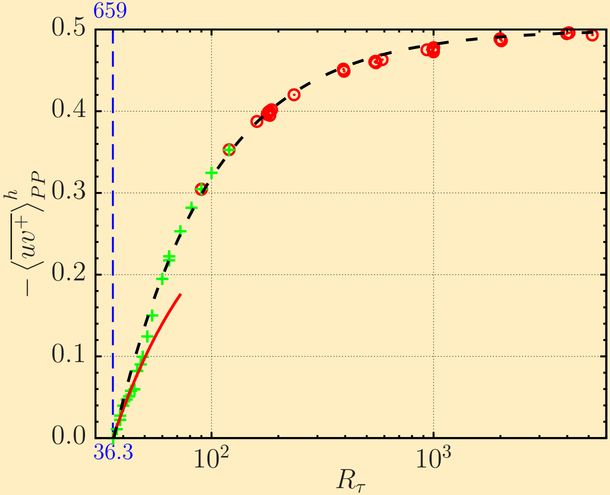

$-\left\langle \overline{u'v'}^{+} \right\rangle_{PP}^{h}$ as a function of R_τ. $(+)$ present DNS. Solid red line from Eq. (2), dashed black line Eq. (3).

Results

Plane Poiseuille flow

- Since

$$\frac{1}{\kappa R_\tau} \ln\left(\frac{R_\tau}{R_{\tau_D}}\right) \leqslant 0.005,$$

- then relation (3) can be limited to

$$\left\langle \overline{u'v'}^{+} \right\rangle_{PP}^{h} = \frac{1}{2}\left(1 - \frac{R_{\tau_C}}{R_\tau}\right) \tag{4}$$

- and leads to the same critical Kármán number $R_{\tau_C} = 36.3$.
- and this, even if the points below $R_{\tau_D} = 174$ do not follow this law. ► ◄

Is this the case for the other flows?

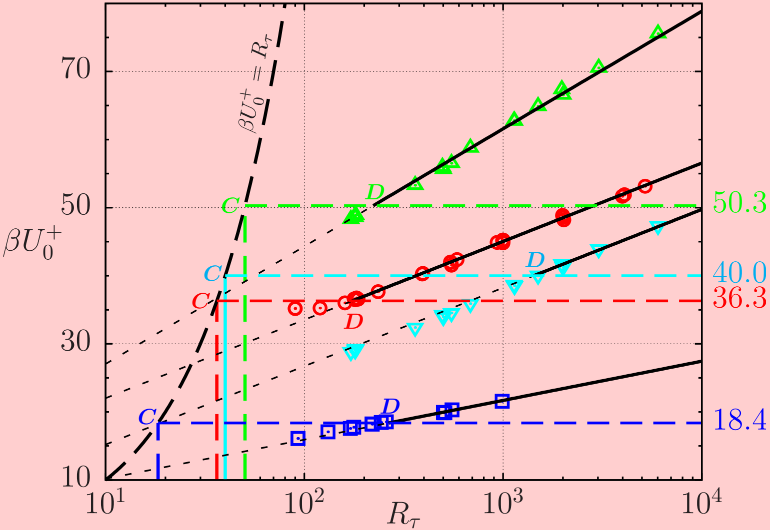

$\boldsymbol{\beta U_0^+}$ as a function of $\boldsymbol{R_\tau}$. Solid line log. law; long-dashed line Laminar curve. ($\boxdot$) ***PC***; ($\bigtriangledown$) ***PF^R***; ($\odot$) ***PP***; ($\bigtriangleup$) ***PF^S***

Results

Is this the case for other flows?

- The same behaviors are observed, namely
  - The product βU_0^+ decreases with $R\tau$ lower than the critical value of each flow represented by the horizontal lines passing through C and D,with

$$\beta U_{0_C}^+ = \beta U_{0_D}^+ = R_{\tau C}.$$

  - It follows a logarithmic law beyond R_{τ_D}, specific to each flow, with RD in the range $\pm 1\%$.
  - Equation (3) therefore applies to the three flows:

$$-\left\langle \overline{u'v'}^+ \right\rangle = \alpha \left[1 - \frac{R_{\tau C}}{R_\tau} - \frac{\beta}{\kappa R_\tau} \ln \left(\frac{R_\tau}{R_{\tau_D}} \right) \right]. \qquad (5)$$

Results

Is this the case for other flows?

- The same behaviors are observed, namely
  - The product βU_0^+ decreases with $R\tau$ lower than the critical value of each flow represented by the horizontal lines passing through C and D, with

$$\beta U^+_{0_C} = \beta U^+_{0_D} = R_{\tau C}.$$

  - It follows a logarithmic law beyond R_{τ_D}, specific to each flow, with RD in the range $\pm 1\%$.
  - Equation (3) therefore applies to the three flows:

$$-\left\langle \overline{u'v'}^+ \right\rangle = \alpha \left[1 - \frac{R_{\tau C}}{R_\tau} - \cancel{\frac{\beta}{\kappa R_\tau} \ln\left(\frac{R_\tau}{R_{\tau_D}}\right)} \right]. \quad (6)$$

For the three flows

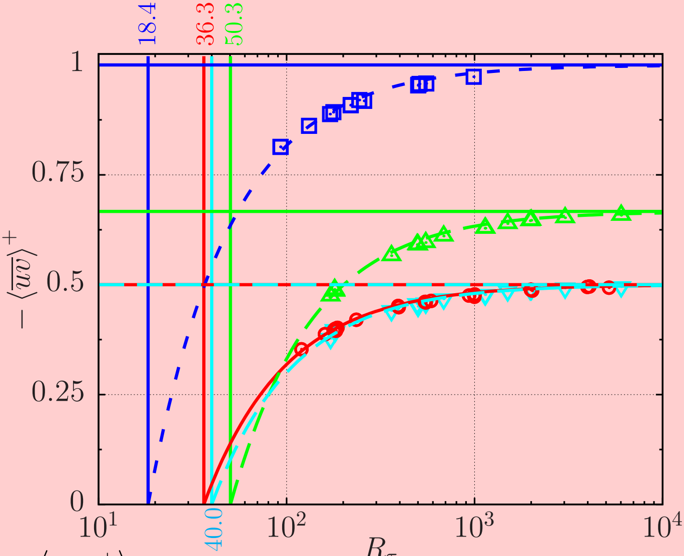

$-\left\langle\overline{\boldsymbol{u'v'}}^+\right\rangle$ vs $\boldsymbol{R_\tau}$. ($\boxdot$) ***PC***; ($\triangle$) ***PF^S***; ($\triangledown$) ***PF^R***; ($\odot$) ***PP***

Results

For the three flows

- This figure shows the evolution as a function of the Kármán number of the bulk-averaged Reynolds shear-stress for the three flows. The critical Kármán numbers are obtained by fitting the data to the simplified function

$$-\left\langle \overline{u'v'}^{+} \right\rangle = \alpha \left(1 - \frac{R_{\tau c}}{R_{\tau}} \right).$$

Flow type	$R_{\tau c}$	R_{0c}	R_{bc}	$R_{\tau D}$	A
PC	18.3	337	337	265	0.17
PP	36.3	659	878	174	0.122
PF^S	50.3	2530	2530	222	0.27
PF^R	40	1600	2133	1423	0.478

Conclusion

- In conclusion, an answer is provided to the question that Reynolds asked one hundred and twenty-five years ago: *Is it possible to obtain a criterion on the critical Reynolds number of the onset of turbulence from the RANS equations?*
- The answer is yes, this criterion is provided by the evolution of the bulk-averaged mean turbulent momentum flux as a function of the Kármán number.
- The critical numbers for canonical internal wall bounded flows are in good agreement with the results available in the literature and listed in table 1.

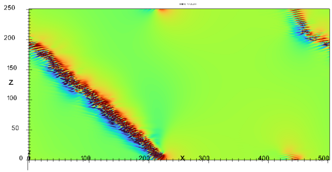

38

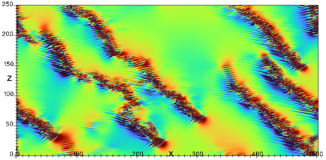

41.5

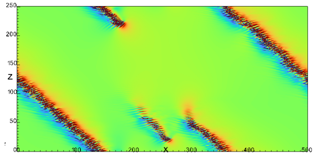

39

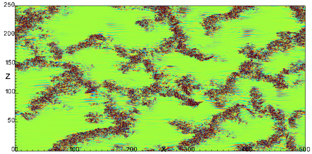

49

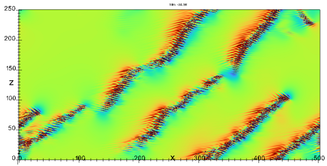

41

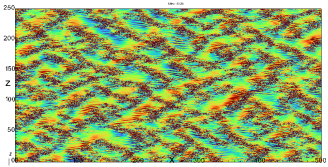

64

Fluctuating streamwise vorticity for (top view)

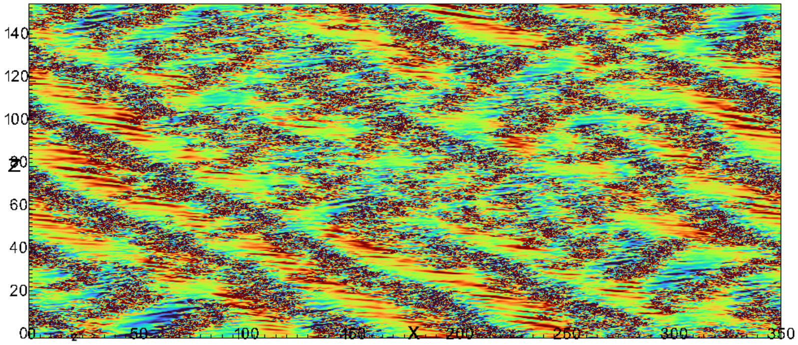

Fluctuating streamwise vorticity for $\boldsymbol{R_\tau} = 72$ (top view)

Thank you, do you have any questions?

Visualisations ($L_x = 225h,\ L_z = 125h$) - $R_b = 760$ ▶

Bibliographie I

AVILA, K., MOXEY, D., DE LOZAR, A., AVILA, M., BERKLEY, D. & HOF, B. 2011 The onset of turbulence in pipe flow. *Science* **333** (6039), 192–196.

AVSARKISOV, V., HOYAS, S., OBERLACK, M. & GARCÍA-GALACHE, J. P. 2014 Turbulent plane Couette flow at moderately high Reynolds number. *Journal of Fluid Mechanics* **751**.

BARKLEY, DWIGHT, SONG, BAOFANG, MUKUND, VASUDEVAN, LEMOULT, GRÉGOIRE, AVILA, MARC & HOF, BJÖRN 2015 The rise of fully turbulent flow. *Nature* **526**, 550 EP –.

BAUER, C., FELDMANN, D. & WAGNER, C. 2017 On the convergence and scaling of high-order statistical moments in turbulent pipe flow using direct numerical simulations. *Physics*

Bibliographie II

BERNARDINI, M., PIROZZOLI, S. & ORLANDI, P. 2014 Velocity statistics in turbulent channel flow up Re_τ=4000. *Journal of Fluid Mechanics* **742**, 171–191.

BOTTIN, S., DAVIAUD, F., MANNEVILLE, P. & DAUCHOT, O. 1998 Discontinuous transition to spatiotemporal intermittency in plane couette flow. *EPL (Europhysics Letters)* **43** (2), 171.

BUFFAT, MARC, LE PENVEN, LIONEL & CADIOU, ANNE 2011 An efficient spectral method based on an orthogonal decomposition of the velocity for transition analysis in wall bounded flow. *Computers & Fluids* **42** (1), 62–72.

CHIN, C., MONTY, J.P. & OOI, A. 2014 Reynolds number effects in DNS of pipe flow and comparison with channels and boundary layer. *International Journal of Heat and Fluid Flow* **45**,

Bibliographie III

DUGUET, Y., SCHLATTER, P. & HENNINGSON, D. S. 2010 Formation of turbulent patterns near the onset of transition in plane couette flow. *Journal of Fluid Mechanics* **650**, 119–129.

ECKHARDT, BRUNO 2018 Transition to turbulence in shear flows. *Physica A: Statistical Mechanics and its Applications* **504**, 121–129.

EL-KHOURY, G. K., SCHLATTER, P., NOORANI, A., FISCHER, P. F., BRETHOUWER, G. & JOHANSSON, A. V. 2013 Direct numerical simulation of turbulent pipe flow at moderately high Reynolds numbers. *Flow, Turbulence and Combustion* **91** (3), 475–495.

FAISST, HOLGER & ECKHARDT, BRUNO 2004 Sensitive dependence on initial conditions in transition to turbulence in

Bibliographie IV

Hoyas, S. & Jiménez, J. 2006 Scaling of the velocity fluctuations in turbulent channels up to $Re_\tau = 2003$. *Physics of Fluids* **18** (1), 011702.

Laadhari, F. 2007 Reynolds number effect on the dissipation function in wall-bounded flows. *Physics of Fluids* **19** (3), 038101.

Laadhari, F. 2019 Refinement of the logarithmic law of the wall. *Phys. Rev. Fluids* **4**, 054605.

Lee, M. & Moser, R. D. 2015 Direct numerical simulation of turbulent channel flow up to $Re_\tau \approx 5200$. *Journal of Fluid Mechanics* **774**, 395–415.

Lee, M. & Moser, R. D. 2018 Extreme-scale motions in turbulent plane Couette flows. *Journal of Fluid Mechanics* **842**, 128–145.

Bibliographie V

MANNEVILLE, PAUL 2015 On the transition to turbulence of wall-bounded flows in general, and plane couette flow in particular. *European Journal of Mechanics - B/Fluids* **49, Part B** (0), 345–362.

MELLIBOVSKY, FERNANDO, MESEGUER, ALVARO, SCHNEIDER, TOBIAS M. & ECKHARDT, BRUNO 2009 Transition in localized pipe flow turbulence. *PRL* **103** (5), 054502.

MUKUND, VASUDEVAN & HOF, BJÖRN 2018 The critical point of the transition to turbulence in pipe flow. *Journal of Fluid Mechanics* **839**, 76–94.

PARANJAPE, CHAITANYA 2019 Onset of turbulence in plane poiseuille flow. PhD thesis, IST Austria.

Bibliographie VI

PIROZZOLI, SERGIO, BERNARDINI, MATTEO & ORLANDI, PAOLO 2014 Turbulence statistics in couette flow at high reynolds number. *Journal of Fluid Mechanics* **758**, 327–343.

PIROZZOLI, SERGIO, ROMERO, JOSHUA, FATICA, MASSIMILIANO, VERZICCO, ROBERTO & ORLANDI, PAOLO 2021 One-point statistics for turbulent pipe flow up to $re_\tau \approx 6000$. *Journal of Fluid Mechanics* **926** (A28), A28.

REYNOLDS, OSBORNE 1883 III. an experimental investigation of the circumstances which determine whether the motion of water shall be direct or sinuous, and of the law of resistance in parallel channels. *Proceedings of the Royal Society of London* **35** (224-226), 84–99.

Bibliographie VII

Reynolds, Osborne 1895 On the dynamical theory of incompressible viscous fluids and the determination of the criterion. *Proceedings of the Royal Society of London. Series A: Mathematical and Physical Sciences* **451** (1941), 5–47.

Wu, Xiaohua & Moin, Parviz 2008 A direct numerical simulation study on the mean velocity characteristics in turbulent pipe flow. *Journal of Fluid Mechanics* **608**, 81–112.

Xiong, Xiangming, Tao, Jianjun, Chen, Shiyi & Brandt, Luca 2015 Turbulent bands in plane-Poiseuille flow at moderate Reynolds numbers. *Physics of Fluids* **27** (4).

Yamamoto, Yoshinobu & Tsuji, Yoshiyuki 2018 Numerical evidence of logarithmic regions in channel flow at $\boldsymbol{Re_\tau} = 8000$. *Physical Review Fluids* **3** (1), 012602–.